

Multi Mode Interferometer for Guided Matter Waves

Erika Andersson¹, Tommaso Calarco², Ron Folman³, Mauritz Andersson⁴, Björn Hessmo⁵, Jörg Schmiedmayer³

¹ Department of Physics, Royal Institute of Technology, SE-10044 Stockholm, Sweden

Department of Physics and Applied Physics, University of Strathclyde, Glasgow G4 0NG, Scotland

² Institut für Theoretische Physik, Universität Innsbruck, A-6020 Innsbruck, Austria

European Centre for Theoretical Studies in Nuclear Physics and Related Areas, 38050 Villazzano (TN) Italy

³ Physikalisches Institut, Universität Heidelberg, D-69120 Heidelberg Germany

⁴ Department of Quantum Chemistry, Uppsala University, S-75120 Uppsala, Sweden

⁵ Dept. of Microelectronics and Information Technology, Royal Institute of Technology, S-164 40 Kista, Sweden

(May 5, 2019)

We describe the fundamental features of an interferometer for guided matter waves based on Y-beam splitters and show that, in a quasi two-dimensional regime, such a device exhibits high contrast fringes even in a multi mode regime and fed from a thermal source.

PACS number(s): 03.75.Be, 03.65.Nk

Interferometers, that is, devices based on the interference of waves propagating in different paths in configuration space, are very sensitive instruments and have provided both insights into fundamental questions and valuable instruments for applications. The sensitivity of matter-wave interferometers [1] has been shown to be much better than that of light interferometers in several areas such as the observation of inertial effects [2]. Because of this high sensitivity, they have to be built in a robust manner to be applicable. This can be achieved by guiding the matter waves and by integration into a single compact device, as has been proven for light optics.

In this Letter, we describe an interferometer for matter waves propagating in a time independent guiding potential, analogous to propagation of light in optical fibers, which has the surprising feature that interference is observed even if many levels in the guide are occupied, and it is fed by a thermal source (for recent micro trap proposals see [3]). This multi mode interferometer (MMI) is built by using two Y-beam splitters (Y-BS) [6] capable of coherently splitting many incoming transverse modes of the guided matter wave, and arranging the interferometer geometry such that all the different transverse states give the same phase shift pattern. The analysis is done in a two-dimensional geometry [4] similar to that existing in solid state electron interferometers [5].

The Y-BS is formed by splitting the atom guiding potential symmetrically into two identical output guides. It was recently demonstrated on an atom chip [6,7] or could be realized based on optical confinement [8]. The symmetric Y-BS enables coherent 50/50 splitting over a wide range of parameters, due to the definite parity of the system [6]. In our simple two dimensional model the beam splitter is modeled by an harmonic potential guide with transverse trapping frequency ω , which is gradually split into two guides, each having $\omega' = 2\omega$, as shown in Fig. 1.b. The BS couples pairs of incoming modes to two spatially separated output modes: In general transverse modes $|2n\rangle$ and $|2n+1\rangle$ from the input guide are connected to transverse modes $|n\rangle_l$ and $|n\rangle_r$ in the two

outgoing guides according to the following rule:

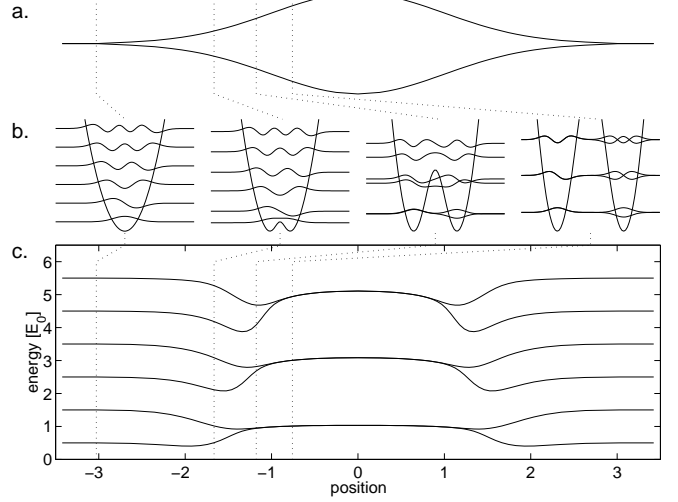


FIG. 1. Basic properties of the guided matter wave interferometer: *a*) Two Y-beam splitters are joined together to form the interferometer. *b*) Transverse eigen-functions of the guiding potentials in various places along the first beam splitter. When the two outgoing guides are separated far enough, i.e. no tunneling between left and right occurs, the symmetric and the anti-symmetric states become degenerate. *c*) Energy eigen-values for the lowest transverse modes as they evolve along the interferometer. One clearly sees that pairs of transverse eigen-states form disjunct interferometers.

$$|2n\rangle \longrightarrow \frac{1}{\sqrt{2}} [|n\rangle_l + |n\rangle_r]$$

$$|2n+1\rangle \longrightarrow \frac{1}{\sqrt{2}} [|n\rangle_l + e^{i\pi} |n\rangle_r].$$

In an ideal symmetric case, coherent splitting for all transverse modes can be achieved [9]. This was confirmed with numerical 2-dim wave packet propagation for the lowest 35 modes.

Similarly, in the case of a Y-BS acting as a recombiner, a superposition of $|n\rangle_l$ and $|n\rangle_r$ will form a superposition of $|2n\rangle$ and $|2n+1\rangle$ in the outgoing guide. For example, an incoming state $\frac{1}{\sqrt{2}}[e^{i\beta/2}|0\rangle_l + e^{-i\beta/2}|0\rangle_r]$ will be recombined to form $\frac{1}{\sqrt{2}}[\cos(\beta/2)|0\rangle + i\sin(\beta/2)|1\rangle]$.

To build an interferometer we join two Y-BS back to back as shown in Fig. 1.a. The first acts as splitter and the second as recombiner. The eigen-energies of the lowest transverse modes along such an interferometer are depicted in Fig. 1.c. From the transverse mode structure one can see that there are many disjunct interferometers in Fock space. Each of them has two input modes ($|2n\rangle$ and $|2n+1\rangle$) and two output modes. In between the Y-BS, the waves propagate in a superposition of $|n\rangle_l$ and $|n\rangle_r$. There will be no transitions between states during the splitting, if the velocity of the transverse guide displacement, as seen by a moving wave packet, is small on the characteristic scale $a_0\omega$ of the transverse guiding potential, where $a_0 \equiv \sqrt{\hbar/(m\omega)}$ is its ground-state size. With this adiabaticity conditions fulfilled, the disjunct interferometers can be discussed separately.

We introduce a phase shift $\Delta\phi$ between the arms by either making one arm longer by Δl ($\Delta\phi = k\Delta l$), where $\hbar k$ represents the momentum along the longitudinal (z) direction, or by applying an additional potential U ($\Delta\phi = \frac{m}{\hbar^2 k} \int U dz$). Both phase shifts are independent of the transverse state in the guide, and they are dispersive. That is, the applied phase shift depends on the incoming k -vector. The dispersion is, to first order in k , the same up to the sign. In the rest of the paper we will use the phase shift caused by a path length difference Δl .

An incoming even state $|2n\rangle$ evolves then into the state $\frac{1}{\sqrt{2}}[e^{i\Delta\phi/2}|n\rangle_l + e^{-i\Delta\phi/2}|n\rangle_r]$ inside the interferometer. When recombined at the second BS it becomes $\frac{i}{\sqrt{2}}[\cos(\Delta\phi/2)|2n\rangle + i\sin(\Delta\phi/2)|2n+1\rangle]$. For an incoming odd state $|2n+1\rangle$ one gets $\frac{i}{\sqrt{2}}[i\sin(\Delta\phi/2)|2n\rangle + \cos(\Delta\phi/2)|2n+1\rangle]$. In general we can describe such an interferometer in terms of a simple matrix

$$A = \begin{pmatrix} A_1 & iA_2 \\ iA_2 & A_1 \end{pmatrix},$$

in the basis of the two incoming and outgoing transverse eigen-modes $|2n\rangle$ and $|2n+1\rangle$, where $A_1 = \cos(\Delta\phi/2)$ and $A_2 = \sin(\Delta\phi/2)$ are the amplitudes which couple the incoming modes to the outgoing ones. This matrix A may in turn be compared to an analogous matrix describing the Mach-Zehnder interferometer in the spatial basis.

Let us discuss the behavior of matter waves in such an interferometer. We start with the simplest case, a wave-packet (WP) of very slow atoms entering in the transverse ground state, and make our way up to the multi mode properties of such an interferometer configuration. Consider a very cold WP occupying the transverse ground state of the incoming guide, with kinetic energy $E_{kin} = k^2\hbar^2/2m$. The wave is split at the first BS and occupies the two ground states of the two inter-

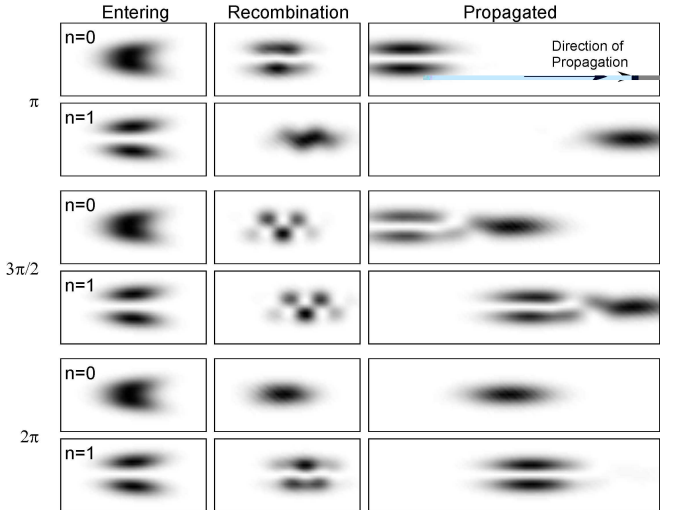


FIG. 2. Basic properties of a wave packet propagating through a guided matter wave interferometer for $|0\rangle$ and $|1\rangle$ incoming transverse modes, calculated by solving the time-dependent Schrödinger equation in two dimensions [10] for realistic guiding potentials. The probability density of the wave function just before entering, right after exiting the interferometer and after a rephasing time t are shown for various phase shifts π , $\frac{3\pi}{2}$ and 2π . One clearly sees the separation of the two outgoing packets due to the energy conservation in the guide, as described in the text. The slight miss alignment between $|0\rangle$ and $|1\rangle$ comes from the different propagation velocities inside the interferometer.

ferometer arms. In the case $E_{kin} < \frac{1}{2}\hbar(\omega' - \omega) = \frac{1}{2}\hbar\omega$ the propagating wave will be reflected already at the first BS. For $E_{kin} > \frac{1}{2}\hbar\omega$, if the WP experiences a phase shift $\Delta\phi \neq 2N\pi$ in one of the arms part of it will, after the recombination at the second BS, attempt to go into the first excited state $n = 1$ of the outgoing guide. In the case $\frac{1}{2}\hbar\omega < E_{kin} < \hbar\omega$, the transition will be forbidden, and these parts will be reflected, while others continue into the outgoing ground state. In the case of a $(2N+1)\pi$ phase shift, the WP will be totally reflected. This back scattering is an interference effect as the zero signal in the outgoing guide is due to the destructive interference for the outgoing $n = 0$ state.

If the kinetic energy of the WP fulfills $E_{kin} \gg \hbar\omega$, transitions to the first excited transverse state at the recombination BS are possible, and no sizeable back reflection occurs. The interference pattern can be observed by looking at the populations in the $|0\rangle$ and the $|1\rangle$ state in the outgoing guide. Again, for an odd – i.e., $\Delta\phi = (2N+1)\pi$ – phase shift, the recombined state will emerge as the first excited state of the outgoing guide. For an even ($2N\pi$) phase shift the outgoing state will be in the ground state $|0\rangle$.

Let us now send into the interferometer a $|0\rangle$ WP with a very small longitudinal energy spread $\Delta E < \hbar\omega$. To separate the two outgoing states we can take advantage of the fact that the part of the WP which makes the transi-

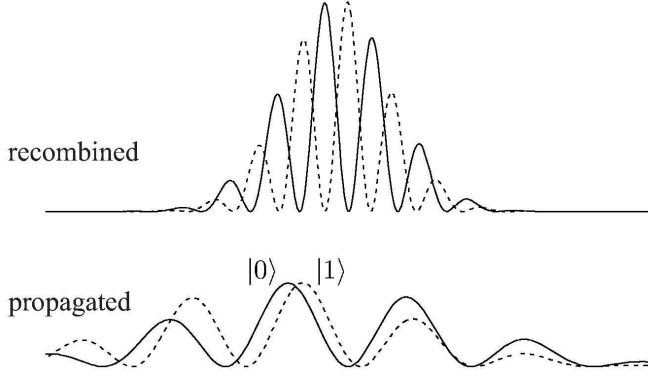


FIG. 3. Schematics of the re-phasing of the interference patterns created by a wave packet entering in an even state $|2n\rangle$ (The WP width is chosen to have more than 2π phase shift difference between its beginning and end). The top graph shows the WP just after recombination at the end of the interferometer, the lower graph after propagation.

tion to the $|1\rangle$ state will lose kinetic energy to compensate for the $\hbar\omega$ additional transverse energy needed for the transition. Therefore the part of the wave packet in the upper state will propagate slower by $\Delta v \simeq \hbar/(mka_0^2)$ than in the lower state. The two outgoing wave packets will become separated (See Fig. 2). Similarly, a WP entering in the first excited transverse state $|1\rangle$, acquiring an odd phase shift $(2N+1)\pi$, will drive towards the $|0\rangle$ state, thus gaining potential energy, propagate faster with Δv and become separated (Fig. 2). To observe this separation between the two outgoing parts of the WP, one has to introduce a pulsed source, which is what we will assume from now onwards.

The above reasoning is easily extended to each of the disjunct interferometers connecting two input modes to two output modes. Components of a WP which acquire an even phase shift will exit in the same transverse state as coming in, while components acquiring an odd phase shift will exit in the complementary transverse state ($|2n\rangle \rightarrow |2n+1\rangle$, or $|2n+1\rangle \rightarrow |2n\rangle$), lose (gain) kinetic energy accordingly and propagate slower (faster) by the *same* Δv . Therefore all interferometers behave similarly and multi transverse mode operation can be expected.

If the energy spread of the WP is large enough ($\Delta k \gg \pi/\Delta l$) a longitudinal interference pattern will form within each of the transverse states as shown in Fig. 3. The two density patterns, at the exit of the interferometer, will add up to the same WP shape one would expect if the interferometer was not there [11]. Looking at the total WP (i.e. not differentiating between the different transverse levels), one only sees its envelope. The two transverse states will propagate with different velocities, as outlined above, and after some time they will "re-phase" as shown in Fig. 3. This will happen once enough time has passed for $|\Delta v|$ to overcome the difference in the position of the pattern peaks at the exit of the interferometer. Since

$|\Delta v|$ is independent of the incoming transverse mode all patterns will re-phase at the same time and position, and thus a multi mode coherent operation has been achieved.

The above principles and the effect of operating the interferometer with an incoherent thermal source can be illustrated within the following simple analytical model. Starting from the momentum representation of the WP $\Psi_{n,k_0}(x, z, t) = \varphi_n(x) \int_{-\infty}^{\infty} dk A_{k_0}(k) e^{ikz} e^{-iEt/\hbar}$, where $\varphi_n(x)$ is the transverse eigen-function $|n\rangle$ in the guide, one finds the wave function after recombination:

$$\Psi_{n,k_0}(x, z, t) = \int_{-\infty}^{\infty} dk A_{k_0}(k) e^{ik_{\pm}l} e^{-iEt/\hbar} \times \left[\varphi_n(x) \cos(k_{\pm}\Delta l/2) e^{ik(z-l)} + i\varphi_{n\mp 1}(x) \sin(k_{\pm}\Delta l/2) e^{ik'_{\pm}(z-l)} \right],$$

where l is the interferometer length (source positioned at beginning of interferometer), and where we used the corrected momenta $k_{\pm} \equiv (k^2 \pm a_0^{-2})^{1/2}$ and $k'_{\pm} \equiv (k^2 \pm 2a_0^{-2})^{1/2}$ to describe the kinetic energy in the interferometer and in the out-going guide. Integrating over the transverse direction and setting $A'_{k_0}(k) = A_{k_0}(k) e^{ik_{\pm}l}$, we find the total longitudinal intensity pattern

$$P_{k_0}^{\pm}(z, t) \equiv |\Psi_{n,k_0}(x, z, t)|^2 = \left| \int_{-\infty}^{\infty} dk A'_{k_0}(k) \cos(k_{\pm}\Delta l/2) e^{ik(z-l)} e^{-iEt/\hbar} \right|^2 + \left| \int_{-\infty}^{\infty} dk A'_{k_0}(k) \sin(k_{\pm}\Delta l/2) e^{ik'_{\pm}(z-l)} e^{-iEt/\hbar} \right|^2.$$

The transverse cross-terms vanish, since the corresponding eigen-functions are orthonormal. Note that the above equation no longer depends on n , except for the sign of the momentum change, which is $(-1)^{n-1}$, i.e. the inverse of the parity of the initial wave function. The expected periodicity can be found by carrying out the cosine integral. One then finds that for an initially narrow width of the source WP and sufficiently long propagation times, the out-going WP behaves like $\cos^2[m\Delta lz/(2\hbar t)]$.

We use this analytical model, which reproduces all the above physics, to discuss the interferometer fed by a statistical mixture of incoming states. As the most general case we imagine a thermal atomic cloud trapped in both transverse and longitudinal directions, with transverse confinement by the same trapping frequency ω as in the incoming guide. In the longitudinal direction, the initial trap is approximated by an infinitely high box of width L . At time $t = 0$, one wall of the box is opened up and the longitudinal states $|\Phi_m\rangle$ start propagating in the positive z direction according to their momentum distributions. The density matrix is $\rho = Z e^{-\beta H} = Z \sum_{m,n=0}^{\infty} e^{-\beta(E_m+E_n)} |\Phi_m\rangle \langle \Phi_m| \otimes |n\rangle \langle n|$, where $Z = 1/\text{Tr}\{e^{-\beta H}\}$. The emergence of an interference pattern, despite the incoherent sum over the transverse and longitudinal states, is confirmed by a numerical calculation.

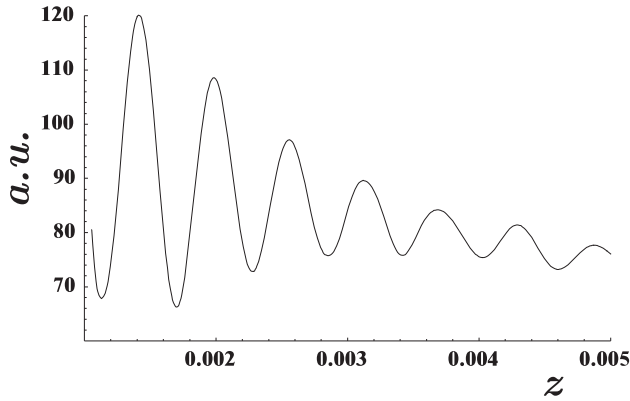


FIG. 4. The longitudinal interference pattern (Li atoms) as a function of z . The interferometer is 1 mm long with the source at its beginning. $\omega = 0.1$ MHz and $L = 100$ μm . $\Delta l = 2$ μm . The time elapsed since the release of the atoms from the trap is 20 ms. The periodicity of the interference pattern is about 550 μm in agreement with the formula $\cos^2[m\Delta l z/(2\hbar t)]$ derived in the text. The length of the interferometer, and the velocity changes occurring already after the first BS, have been included in the calculation.

Figure 4 gives an example for an interference pattern obtained with a typical ‘hot’ atom ensemble with a temperature of 200 μK and guides with a trap frequency of 10^5 Hz, already realized on an Atom Chip [12,13]. Even though this leads to a population of hundreds of transverse levels, high contrast fringes are observed. It is interesting to note that although the coherence length of the thermal state is in the order of the de Broglie wave length ($\lambda_{dB} \sim 0.1$ μm), a path length difference of 2 μm still enables a coherent overlap between the two arms. This is due to the pulsed nature of the experiment, which results in a small velocity uncertainty δv of the detected atoms and consequently to a much longer coherence length. Typical position detection resolution achieved on the Atom Chip and millisecond evolution times over mm distances allow for coherence on a length scale $> 50\lambda_{dB}$.

To summarize, we have shown that a multi-mode interferometer may be realized in a two dimensional geometry by making use of the symmetric Y- beam splitter. Furthermore, though beyond the scope of the present work, we expect three dimensional evolution to also exhibit qualitatively the same behavior under certain conditions. As such Y-beam splitters have been realized, we expect the road to be open for the experimental realization of robust guided matter wave interferometers.

We would like to thank Peter Zoller for enlightening discussions. R.F. is grateful to Joseph Imry for his insight into mesoscopic systems. E.A. would like to thank Helmut Ritsch for his kind hospitality. This work was supported by the Austrian Science Foundation (FWF), project SFB S065-05, F15-07, by the Istituto Trentino di Cultura (ITC) and by the European Union,

contract Nr. IST-1999-11055 (ACQUIRE), HPMF-CT-1999-00211 and HPMF-CT-1999-00235.

-
- [1] *Proceedings of the International Workshop on Matter Wave Interferometry*, ed. by G. Badurek, H. Rauch, and A. Zeilinger [Physica (Amsterdam) **151B**, No. 1-2 (1988)]; *Atom Interferometry*, ed. by P. Berman, Academic Press (1997).
 - [2] For example see: A. Peters, Keng Yeow Chung and S. Chu, Nature **400**, 849 (1999); T.L. Gustavson, A. Landragin and M.A. Kasevich, J. Class. and Quant. Grav. **17**, 2385 (2000); and references there in.
 - [3] Recently, several proposals for matter-wave interferometers have been made in the context of splitting and combining a microtrap ground state with a time dependent potential: E.A.Hinds, C.J. Vale and M.B.Boshier, Phys. Rev. Lett. **86**, 1462 (2001); W. Hänsel, J. Reichel, P. Hommelhoff and T.W.Hänsch, quant-ph/0106162.
 - [4] In 2d confinement the out of plane transverse dimension is either subject to a much stronger confinement or can be separated out. For an experimental realization see: H. Gauck *et al.* Phys. Rev. Lett. **81**, 5298 (1998); T. Pfau priv. comm. (2000); Other proposals: E.A. Hinds, M.G. Boshier, I.G. Hughes Phys. Rev. Lett. **80**, 645 (1998); R.J.C. Spreeuw, *et al.* Phys. Rev. A **61**, 053604 (2000).
 - [5] E. Buks *et al.*, Nature **391**, 871-874 (1998).
 - [6] D. Cassettari, B. Hessmo, R. Folman, T. Maier, J. Schmiedmayer, Phys. Rev. Lett. **85**, 5483 (2000).
 - [7] D. Müller, *et al.*, Phys. Rev. A **63**, 041602(R) (2001).
 - [8] O. Houde *et al.*, Phys. Rev. Lett. **85**, 5543 (2000).
 - [9] This is an advantage over four way beam splitter designs relying on tunneling through a barrier between two guides – see E. Andersson, M. T. Fontenelle, and S. Stenholm, Phys. Rev. A **59**, 3841 (1999). Here, the splitting ratios for incoming wave packets are very different for different transverse modes, since the tunneling probability depends strongly on the energy of the particle. Even for single mode the splitting amplitudes, determined by the barrier width and height, are extremely sensitive to experimental noise.
 - [10] The numerical code is based on a Split-Operator formalism with a pseudospectral method for derivatives see e.g. M. Feit, J. Fleck Jr, and A. Steiger, J. Comput. Phys. **47**, 412 (1982); B. M. Garraway, K.-A. Souminien, Rep. Prog. Phys. **58**, 365 (1995).
 - [11] This is only approximately true, because inside the IFM there are different propagation velocities due to the different potential energies of even and odd incoming states. In the calculations this small effect is included.
 - [12] R. Folman *et al.*, Phys. Rev. Lett. **84**, 4749 (2000); current traps on our chips achieve $\omega > 1$ MHz.
 - [13] For other Atom Chip experiments see: J. Reichelet *et al.*, Phys. Rev. Lett. **83**, 3398 (1999); D. Müller *et al.*, Phys. Rev. Lett. **83**, 5194 (1999); N.H. Dekker, *et al.*, Phys. Rev. Lett. **83**, 3398 (1999).